Mon. Not. R. Astron. Soc. **390,** 819–828 (2008) doi:10.1111/j.1365-2966.2008.13792.x

The Combined NVSS–FIRST Galaxies (CoNFIG) sample – I. Sample definition, classification and evolution

M. A. Gendre⋆ and J. V. Wall⋆

Department of Physics and Astronomy, The University of British Colombia, 6224 Agricultural Road, Vancouver, BC, Canada V6T 1Z1

Accepted 2008 July 31. Received 2008 July 31; in original form 2008 May 8

ABSTRACT

The CoNFIG (Combined NVSS–FIRST Galaxies) sample is a new sample of 274 bright radio sources at 1.4 GHz. It was defined by selecting all sources with $S_{1.4\,\mathrm{GHz}} \geq 1.3$ Jy from the NRAO Very Large Array (VLA) Sky Survey (NVSS) in the north field of the Faint Images of the Radio Sky at Twenty centimetres (FIRST) survey. New radio observations obtained with the VLA for 31 of the sources are presented. The sample has complete Fanaroff–Riley (FRI)/FRII morphology identification; optical identifications and redshifts are available for 80 and 89 per cent of the sample, respectively, yielding a mean redshift of ∼0.71. One of the goals of this survey is to get better definitions of luminosity distributions and source counts of FRI/FRII sources separately, in order to determine the evolution of the luminosity function for each type of source. We present a preliminary analysis, showing that these data are an important step towards examining various evolutionary schemes for these objects and to confirm or correct the dual population unified scheme for radio active galactic nuclei (AGN). Improving our understanding of radio galaxy evolution will give better insight into the role of AGN feedback in galaxy formation.

Key words: surveys – galaxies: active – galaxies: luminosity function, mass function – galaxies: statistics – radio continuum: galaxies.

1 INTRODUCTION

Longair (1966) determined that powerful radio sources undergo strong differential evolution, the first indication of cosmic downsizing. Since then our understanding of the space density of active galactic nuclei (AGN) as a function of cosmic epoch has steadily continued to advance.

With the development of evolutionary models for radio sources came the idea of a dual-population model. The initial version of this dichotomy (Longair 1966) was in terms of low and high luminosities. But with high-frequency surveys, and the large number of flat/inverted spectrum sources revealed in them, an alternative classification emerged, based exclusively on the source spectra: sources with a spectral index $\alpha \leq -0.5$ (where $S_\nu^\alpha \propto \nu^\alpha$), corresponding to optically thin synchrotron radiation, were classified as steep spectrum, whereas sources with lower spectral indices ($\alpha \geq -0.5$) inevitably showed features of synchrotron self-absorption and were classified as flat spectrum. Initial indications suggested that these two populations underwent different evolution (Schmidt 1976; Masson & Wall 1977). However, Dunlop & Peacock (1990) studied the radio luminosity function (density of sources with a given luminosity per unit of comoving volume) of these two classes of radio sources, and came to the conclusion that both populations were undergoing a similar evolution, implying that they might not actually be distinct.

The Fanaroff–Riley (FR) classification (Fanaroff & Riley 1974), originally a subclassification for steep-spectrum objects, was employed to provide a further categorization of radio sources. This classification divides radio sources into two classes of double-lobed sources based on the appearance of their jets. The FR type I (FRI) objects have the highest brightness along the jets and core, reside in moderately rich cluster environments (Hill & Lilly 1991) and include sources with irregular structure (Parma et al. 1992). In contrast, FRII sources show hotspots in the lobes and more collimated jets, are found in more isolated environments and display stronger emission lines (Baum & Heckman 1989; Rawlings et al. 1989). Fanaroff & Riley (1974) found these two classes to be divided in radio power, with a break luminosity $P_{178\,\mathrm{MHz}} \sim 10^{25}\,\mathrm{W\,Hz^{-1}\,sr^{-1}}$, with FRII sources lying above this limit. Subsequently Owen & Ledlow (1994) showed that the break was a function of both radio and optical luminosity.

During the 1980s the 'unification' hypothesis emerged to describe how viewing aspect could relate radio quasi-stellar objects (RQSOs) of either flat or steep spectrum to FRII radio galaxies (e.g. Peacock 1987; Scheuer 1987; Barthel 1989). However, the scheme did not include lower luminosity AGN such as FRI galaxies and BL Lac objects. The unifying connection between these was

⋆E-mail: mgendre@phas.ubc.ca (MAG); jvw@phas.ubc.ca (JVW)

introduced by Marcha & Browne (1995). The unified model of AGN proposed by Wall & Jackson (1997) and Jackson & Wall (1999) assumes that the cosmic evolution of radio-loud AGN is based on a division of the radio sources into a low-luminosity ($P_{178\,\mathrm{MHz}} < 10^{25}\,\mathrm{W\,Hz^{-1}\,sr^{-1}}$) component corresponding to FRIs, and a high-luminosity component corresponding to FRIIs. In this scheme, the various forms of AGN observed (FRI and FRII extended double sources, flat- and steep-spectrum RQSOs and BL Lac objects) result from the orientation of the extended parent objects with respect to the observer's line of sight. Indeed, because the double-sided ejection of synchrotron blobs in AGN is at relativistic speed, the orientation of the ejection axis to the line of sight becomes crucial: sources viewed side-on appear as double radio galaxies (FRI or FRII) and sources viewed along the jets appear as RQSOs (beamed counterparts of FRII sources) or BL Lac objects (beamed counterparts of FRI sources). The relativistically boosted jet emission in the beamed counterparts of the extended sources dominates the extended emission, making the overall radio emission appear compact down to very long baseline interferometry (VLBI) scales.

Initially, in modelling the space density of radio AGN, it was assumed for simplicity that the low-luminosity radio galaxies including FRI sources showed no cosmic evolution (Wall, Pearson & Longair 1980; Jackson & Wall 1999), the strong cosmic evolution confined only to the higher luminosities and the FRII galaxies. With the advent of large-scale redshift surveys for nearby galaxies, many authors, including Brown, Webster & Boyle (2001), Snellen & Best (2001), Willott et al. (2001), Sadler et al. (2007) and Rigby, Best & Snellen (2007), found significant evolution for low power sources – but mild evolution in comparison with that of the high-luminosity sources. Rigby et al. (2007) argued that if both FRIs and FRIIs have similar evolution, the dual-population scheme could be reduced to a single-population model.

The FRI/FRII dual-population scheme has encountered several problems. One of these concerns the correspondence between FRI galaxies and BL Lac objects. Urry & Padovani (1995) noted that some BL Lac objects have non-FRI-like morphologies and that the density of FRI sources is too low to account for the entire BL Lac population, a concern also raised by Wall & Jackson (1997). Looking at BL Lac objects from another point of view, Marcha et al. (1996) demonstrate that only about one-third of low-luminosity core-dominated radio sources – which are supposedly the beamed counterpart of FRI sources – are conventional BL Lac objects. Most of the remaining sources have optical classification such as Seyfert objects or elliptical galaxies.

A related issue concerns the existence of FRI RQSOs. Until recently, these objects were thought not to exist, leading to the hypothesis that FRI and FRII central engines were of different nature (Baum, Zirbel & O'Dea 1995) and that the torus opening in FRI sources was too small to observe a quasar nucleus (Falcke, Gopal-Krishna & Biermann 1995). However, the discovery of an FRI QSO, E1821+643, by Blundell & Rawlings (2001) overthrew those assumptions. More recent Very Large Array (VLA) observations (Heywood, Blundell & Rawlings 2007) uncovered another four sources of this type.

Finally, if sources with different FR classes undergo different evolution, this might imply that their fundamental characteristics, such as the black hole spin or jet composition, are different too. However, the existence of hybrid sources, which display both FRI and FRII morphological characteristics (Capetti et al. 1995), then becomes puzzling. Based on observations of hybrid sources, Kaiser & Alexander (1997) argued that the FR dichotomy is based purely on the interaction between the jets and the environmental medium, and not on intrinsic properties of the central engine. This view is also supported by Gopal-Krishna & Wiita (2000) and Gawronski et al. (2006). However, Wang et al. (1992) suggested that some AGN engines could be capable of ejecting jets of unequal power, resolving the problem of hybrid sources. Gopal-Krishna & Wiita (2000) found no evidence for such a process in their sample.

Other schemes have been suggested to resolve these difficulties. Kaiser & Best (2007) explained the FR dichotomy by postulating that all sources start as FRII objects and used an analytical model in which the evolution of the radio sources is governed by energy losses from both radiating relativistic electrons in the lobes and turbulence in the jets.

Willott et al. (2001) used an approach to a dual-population unified scheme based on the luminosity of sources instead of morphology. Optical spectra of FRII sources are heterogeneous and they can display both strong and weak low-excitation emission lines (Laing 1994). Therefore, radio sources can also be grouped based on their emission lines, with one population composed of low-luminosity sources having weak emission lines (containing both FRI and FRII objects), and the other composed of high-luminosity sources with strong emission lines (containing only FRII objects). With this model, Willott et al. (2001) concluded that high-luminosity objects undergo a stronger evolution with epoch than low-luminosity sources, as found by e.g. Longair (1966), Wall et al. (1980) and Urry & Padovani (1995), and that the radio luminosity function has the form of a broken power law, similar to the conclusions of Dunlop & Peacock (1990). We note that, since conventional accretion disc systems are expected to be strong X-ray sources, luminosity-based dual-population models are also used in modelling the luminosity function of X-ray selected RQSOs (Hardcastle, Evans & Croston 2006).

Defining the relation between the different radio subpopulations together with their cosmic evolution is becoming fundamental to our understanding of galaxy formation.

The current paradigm for galaxy formation follows hierarchical build-up in a cold dark matter (CDM) universe. Nevertheless, serious difficulties arise from this model in its simplest form, as discussed by Bower et al. (2006). It implies that current epoch galaxies must be the largest and bluest and have the highest star-forming rate of all galaxies. Observations show that they are red, old galaxies, whereas the bulk of star formation is observed at earlier epochs. This is known as downsizing, first described by Cowie et al. (1996). AGN negative feedback could be the key to understanding this phenomenon. The ignition of the nucleus in a star-forming galaxy could eject the gas into the intergalactic medium, thus reducing or even stopping star formation, breaking the hierarchical build-up (Silk & Rees 1998; Granato et al. 2001; Quilis, Bower & Balogh 2001). Note that there is also some positive AGN feedback (Klamer et al. 2004; van Breugel et al. 2004) in which the pressure from the jets compresses the interstellar medium and induces star formation. The balance between these processes remains to be understood; establishing the cosmic behaviour of the radio AGN is important in revealing the precise role of the feedback mechanisms.

Although FRI and FRII sources show different evolution, they also lie in different luminosity ranges. There is therefore a possibility that both types may show similar evolution for overlapping luminosities (i.e. high-luminosity FRIs and low-luminosity FRIIs). In order to sort out the FR dichotomy and its details, accurate models of the evolution of each population are needed. This implies compiling accurate statistics, such as luminosity distributions and

source counts, for both types separately. This is the goal of the CoNFIG (Combined NVSS–FIRST Galaxies) sample presented here, a new sample of bright radio sources with complete morphological identification.

The CoNFIG sample is defined as all sources with $S_{1.4\,\mathrm{GHz}} \geq 1.3$ Jy from the NRAO VLA Sky Survey (NVSS; Condon et al. 1998) catalogue within the north region of the Faint Images of Radio Sources at Twenty centimetres survey (FIRST; White et al. 1997), a 1.5-sr region defined roughly by $-8^\circ \leq$ Dec. $\leq 64^\circ$ and 7h $\leq$ RA $\leq$ 17 h. The flux density limit of 1.3 Jy was chosen so that the number of sources in the sample was of statistical significance while allowing us to identify the morphology for each source individually. Optical identifications were obtained from the SuperCOSMOS Sky Survey (SSS; Hambly et al. 2001) and redshift information extracted using the SIMBAD data base. With the accompanying VLA observations described here, the sample has complete morphology information, a median flux density of $S_{1.4\,\mathrm{GHz}} \sim 1.96$ Jy and optical identifications and redshift information for ∼80 per cent and ∼89 per cent of the sources, respectively.

The structure of this paper is as follows. The details of the construction of the CoNFIG sample are explained in Section 2 while Section 3 describes how the morphologies were determined. Optical identifications and redshift information are discussed in Section 4 and Section 5 outlines the computation of the morphology-dependent luminosity distributions. Finally, Section 6 describes and discusses the FRI/FRII source counts.

Throughout this paper, we assume a standard ΛCDM cosmology with $H_0 = 70$ km s^{-1} Mpc^{-1}, $\Omega_\mathrm{M} = 0.3$ and $\Omega_\Lambda = 0.7$.

2 THE CONFIG SAMPLE

2.1 Radio Surveys

2.1.1 NVSS

The NVSS is a 1.4-GHz continuum survey covering the entire sky north of -40° declination (corresponding to an area of 10.3 sr). The completeness limit is about 2.5 mJy with an rms brightness fluctuation of about 0.45 mJy beam^{-1}. The survey has yielded over 1.8 million sources, implying a surface density of ∼50 sources per square degree. It was carried out with the VLA in D and DnC configuration (the D configuration being the most compact VLA configuration with a maximum antenna separation of ∼1 km), providing an angular resolution of about 45 arcsec full width at half-maximum (FWHM) (Condon et al. 1998).

Since the median angular size of faint extragalactic sources at these flux density levels is $\lesssim$10 arcsec (Condon et al. 1998), most sources are unresolved, and the NVSS flux density measurements are quite accurate. However, the large beam size does not allow one to determine precise structure of sources or to determine positions accurate enough to establish optical counterparts.

2.1.2 FIRST

The FIRST is another 1.4-GHz continuum survey, covering an area of ∼9030 deg^2 over the North Galactic Pole. The completeness limit is about 1 mJy with a typical rms of 0.15 mJy. The survey yielded ∼811 000 sources, implying a surface density of ∼90 sources per square degree. It was carried out with the VLA in B configuration (the B configuration having a maximum antenna separation of ∼10 km), which provides an angular resolution of about 5 arcsec FWHM (White et al. 1997). This survey complements the NVSS survey well, providing a beam size small enough to resolve the structure of most nearby extended radio sources.

2.2 Sample definition

The CoNFIG sample is defined as all sources with $S_{1.4\,\mathrm{GHz}} \geq 1.3$ Jy from the NVSS catalogue within the north region of the FIRST survey (1.5-sr region defined roughly by $-8^\circ \leq$ Dec. $\leq 64^\circ$ and 7h $\leq$ RA $\leq$ 17 h), resulting in a sample of 261 objects.

Very large sources resolved in NVSS within this initial sample, such as 3CRR sources (Laing, Riley & Longair 1983), need to be considered. In these cases, two or more NVSS sources with $S_{1.4\,\mathrm{GHz}} \geq 1.3$ Jy are actually components of a much larger resolved source. After collecting the resolved source components together, the refined sample contains 248 sources.

Multicomponent sources, where each component has $S_{1.4\,\mathrm{GHz}} <$ 1.3 Jy but with a total flux density $S_{1.4\,\mathrm{GHz}} \geq 1.3$ Jy, also need to be considered. For this purpose, NVSS sources with $0.1 \leq S_{1.4\,\mathrm{GHz}} \leq$ 1.3 Jy were selected and, if any other source in the catalogue was located within 4 arcmin of the listed sources, they were set aside as candidate extended sources. The final decision on whether or not the sources are actually components of a resolved source was made by visual inspection of the NVSS contour plot. In this manner, 32 more sources were added to the sample.

Finally, after looking at the NVSS and FIRST contour plots and optical information of all the sources, seven sources[1] were deleted, either because the source is a globular cluster, or because the source actually consists of independent sources, each with $S_{1.4\,\mathrm{GHz}} <$ 1.3 Jy.

The final sample, referred to as the CoNFIG Sample, consists of 274 sources. Details of the sources can be found in Appendix A.

3 MORPHOLOGY

3.1 Initial classification

76 sources in the sample appear in the 3CRR catalogue (Laing et al. 1983) in which the morphology type of each 3CRR source has been determined. These sources are marked by a star next to their 3C name in Appendix A.

For other sources, the morphology was determined by looking at the FIRST and NVSS radio contour plots, obtained from the NASA virtual observatory Skyview (http://skyview.gsfc.nasa.gov). The contour plots are shown in Appendix C.

If the contour plot displays distinct hotspots at the edge of the lobes (as in Fig. 1), and the lobes are aligned, the source was classified as FRII. On the contrary, sources with collimated jets showing hotspots near the core and jets were classified as FRI (see Fig. 2). Most irregular-looking sources were also classified as FRI (Parma et al. 1992).

Contour plots were obtained for all but one (CoNFIG-225) of the CoNFIG sources. 53 sources were identified as extended but the resolution is too low to confirm their exact morphological types. Additional VLA observations were obtained for 31 of these sources

[1] Note that three of these sources (CoNFIG-015, CoNFIG-076 and CoNFIG-225) were deleted later in the sample construction process, based on the 8-GHz VLA observations described in Section 3.2.

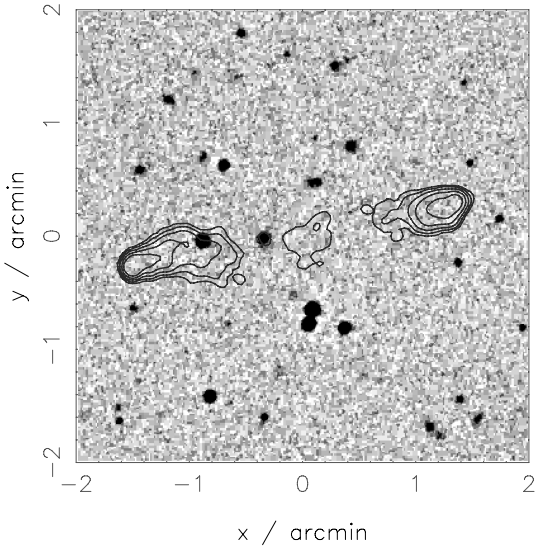

Figure 1. Typical FIRST contour plot of FRI source (here, 3C 284) against SSS grey-scale optical background. The hotspots are located along the jets and more towards the core of the source.

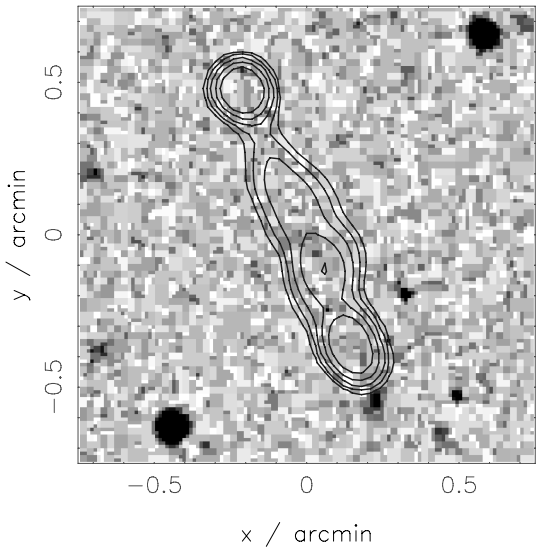

Figure 2. Typical FIRST contour plot of FRII source (here, 3C 223) against SSS grey-scale optical background. The hotspots are located at the edge of the lobes.

(see Section 3.2) while for the other 22 sources, data were found in the VLA archives.

As specified in Section 2.2, seven sources were deleted from the sample after examination of their contour plots. In one case, the source is a globular cluster and in another case, the source has no FIRST or NVSS contours. The other five NVSS 'sources', when observed with FIRST, actually consist of separate and independent sources, each with $S_{1.4\,\mathrm{GHz}} < 1.3$ Jy. The NVSS radio positions of these sources can be found in Table 1.

3.2 VLA observations

Radio observations of 31 extended sources with uncertain morphological classification were taken at 8 GHz using the VLA in A configuration on 2007 July 29. The observations used the standard two IFs of 8435.1 and 8485.1 GHz, with a bandwidth of 50 MHz. The A configuration is the configuration with the largest spacing between antennas (∼36 km), providing a synthesized beam of 0.24 arcsec FWHM at 8 GHz.

The 8-GHz flux density of each source was derived from the 1.4-GHz NVSS flux density and spectral index (see details in Section 5), and the exposure time was computed for each source such as to provide a signal-to-noise ratio of at least 5. The sources were placed accordingly into four different exposure time groups (5, 10, 20 and 30 min), except for CoNFIG-227 (60 min) and CoNFIG-257 (40 min). For observations with a 30-min exposure time, the exposure was split into two separate 15-min scans to improve *uv* coverage. The primary calibrator 3C 174 (0542+498) was observed at the beginning of the run while 3C 286 (1331+305) was observed twice during the run, once in the middle and once at the end. These calibrate the flux density scale assuming a flux density of 4.84 Jy at 8435.1 MHz and 4.81 Jy at 8485.1 MHz for 3C 174 and 5.18 Jy at 8435.1 MHz and 4.99 Jy at 8485.1 MHz for 3C 286, based on the scale of Baars et al. (1977). Nearby secondary calibrators were observed approximately every 30 min to provide phase calibration. Details of the observations are shown in Appendix D.

Table 1. Sources deleted from the original sample.

Source	Reason deleted
08 14 43.59 +12 58 10.0	Two separate sources
08 30 04.12 +07 45 45.0	Two separate sources
10 34 05.09 +11 12 32.1	Two separate sources
12 30 35.69 +12 19 18.2	Globular cluster
13 23 02.33 +29 41 34.0	Three separate sources
14 17 00.49 +07 10 50.2	Two separate sources
15 40 30.42 −05 03 17.4	No contours

3.3 Final classification

Data were extracted from the VLA archives at other frequencies and configurations for some sources for which the 8-GHz contours were not satisfactory. All data were reduced using standard procedures incorporated within the AIPS software provided by NRAO, and the resulting images are grouped in Appendix D.

Over 60 per cent of sources in the CoNFIG sample are classified either as FRI or as FRII. The rest of the sources are classified as compact or deleted from the sample (see Table 1). Some sources in this group will be unresolved high redshift FRIIs, and some others are confirmed as truly compact from the VLBA calibrator list (Beasley et al. 2002; Fomalont et al. 2003; Petrov et al. 2005, 2006; Kovalev et al. 2007) or from the Pearson–Readhead survey (Pearson & Readhead 1988). Some of these confirmed compact sources show a steep ($\alpha \leq -0.6$) spectral index and are possible compact steep sources (CSS) (Fanti & Fanti 1994).

After looking at optical counterparts from the SSS (as discussed in Section 4), two particular subclasses of compact and FRII sources are identified.

(1) Some compact sources show no optical counterpart. These sources can be classified either as CSS or as unresolved FRII. When confirmed as a compact source from the VLBA calibrator list (see Beasley et al. 2002; Fomalont et al. 2003; Petrov et al. 2005, 2006; Kovalev et al. 2007) or the Pearson–Readhead survey (Pearson & Readhead 1988), the source is classified as CSS and is included in

Table 2. Morphology of the sources in the CoNFIG sample. The morphology of each source is determined by looking at FIRST and NVSS contour plots or from VLA observations as described in Sections 3.1 and 3.2, respectively.

FRI	FRII	Unresolved	Compact	CSS
36	135	22	75	6
13.1 per cent	49.3 per cent	8.0 per cent	27.4 per cent	2.2 per cent

Table 3. Details of the extra samples constructed to better define the FRI/FRII source counts. The total number of sources as well as the number of FRI, FRII and unresolved extended, compact and compact steep spectrum sources, are shown here.

	$S_{\rm lim}$ (mJy)	Area (deg^2)	Number of sources FRI	FRII	C	Total
CoNFIG-2	800	2915.25	27	149	67	243
CoNFIG-3	200	370.00	41	205	45	291
CoNFIG-4	50	64.00	42	119	73	234

the compact sources statistics. Otherwise, the source is assumed to be an unresolved FRII. Their inclusion into the FRII group has a low impact on the FRII statistics, as seen in Fig. 6.

(2) Other sources are classified as FRII and present a stellar type optical identification. These sources are – on the basis of the unified model – steep-spectrum RQSOs, which occur when the line of sight of the observer is oriented at less than 45° with respect to the jets, enabling the observer to look inside the dusty torus.

The final classification for each source is shown in Table A and the distribution of morphological types is presented in Table 2. Errors in flux density measurements are well defined for point sources in the catalogues, but corresponding error estimates for the extended sources were too uncertain to be worth including here.

3.4 CoNFIG-2, CoNFIG-3 and CoNFIG-4

In order to improve the FRI/FRII statistics, three more samples of about 250 sources each, and complete to 0.8 Jy (CoNFIG-2), 0.2 Jy (CoNFIG-3) and 50 mJy (CoNFIG-4), were constructed from the NVSS catalogue over various areas, all included in the FIRST northern region. For each sample, the morphologies of the sources were determined as described in Section 3.1. Details of the samples are given in Table 3 while the data for the samples are shown in Tables B1 and B2. Optical identification and redshifts were retrieved for CoNFIG-2 only, as described in the next section.

Because the morphology information is not complete for all sources in the CoNFIG-2, CoNFIG-3 and CoNFIG-4 samples, these objects were only used to compute the FRI/FRII source count (see Section 6.2).

4 OPTICAL IDENTIFICATIONS AND REDSHIFTS

To determine core coordinates in order to retrieve redshifts, optical identifications (together with $B_j, R1, R2$ and I magnitudes) were obtained for 79 per cent of the sources in the CoNFIG sample and 61 per cent of the sources in the CoNFIG-2 sample from the SSS (Hambly et al. 2001).

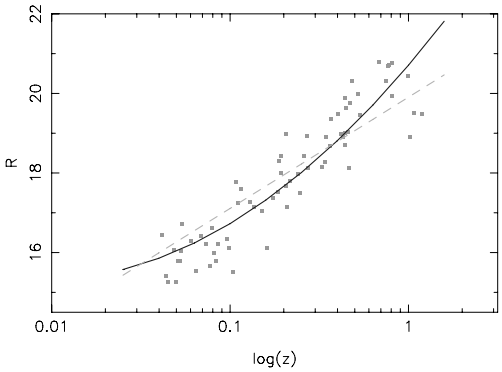

Figure 3. R–z relation from CoNFIG data for extended sources with $15 \leq R \leq 21$. The squares represent objects classified as FRI or FRII (excluding unresolved sources) with optical ID and spectroscopic redshift information. The solid line shows the quadratic fit $[R = 20.70 + 5.24 \log z + 1.28 (\log z)^2]$ from which photometric redshifts are estimated. For comparison, the linear fit is also shown (dashed line).

Redshifts were retrieved for 230 CoNFIG sources and 161 CoNFIG-2 sources, using the SIMBAD (http://simbad.u-strasbg.fr/simbad) and NED (http://nedwww.ipac.caltech.edu/) data bases.

Redshift and magnitude information are listed in Appendix A for CoNFIG, and in Table B1 for CoNFIG-2.

When spectroscopic redshifts were not available, we estimated photometric redshifts via an empirical R–z relation derived from extended sources in the CoNFIG sample with galaxy identifications and $15 \leq R \leq 21$, as shown in Fig. 3. A simple fit to these data is

$$R = 20.70 + 5.24 \log z + 1.28 (\log z)^2. \quad (1)$$

Photometric redshift estimate is given to 14 CoNFIG objects falling into this category, but with no spectroscopic redshift information, bringing the redshift coverage to 244 sources (89 per cent of the sample).

For the CoNFIG sample, redshifts range from $z = 0.0033$ to 3.522 with a mean redshift of $z = 0.715$ and a median redshift of $z = 0.580$. The morphology-dependent distribution is shown in Fig. 4 and details of the redshift distributions are given in Tables 4 and 5. The FRI distribution is concentrated at low redshifts ($z \leq 0.5$) while the FRII distribution covers a wider range, up to $z = 2.5$.

Note that for 38 CoNFIG and 34 CoNFIG-2 sources, redshift information was retrieved from the literature using the radio position of the object, but no counterpart was found in SSS.

5 LUMINOSITY DISTRIBUTIONS

In order to compute the radio luminosity, the spectral index α (defined as $S_\nu \propto \nu^\alpha$) of each source needs to be determined. To achieve this, flux densities at different frequencies for each source were compiled and the spectral index computed following the relation

$$\alpha = \frac{\Delta \log(S)}{\Delta \log(\nu)}. \quad (2)$$

A summary of the different frequencies and corresponding surveys used to retrieve the flux density information is given in Table 6.

We made independent estimates for the low- and high-frequency spectral indices (with 178 MHz $\leq \nu \leq$ 1.4 GHz and 1.4 $\leq \nu \leq$ 5 GHz, respectively). The low-frequency spectral indices are used to compute the luminosities; since $\nu_{\rm rest} = \nu_{\rm obs}(z + 1)$, the luminosity

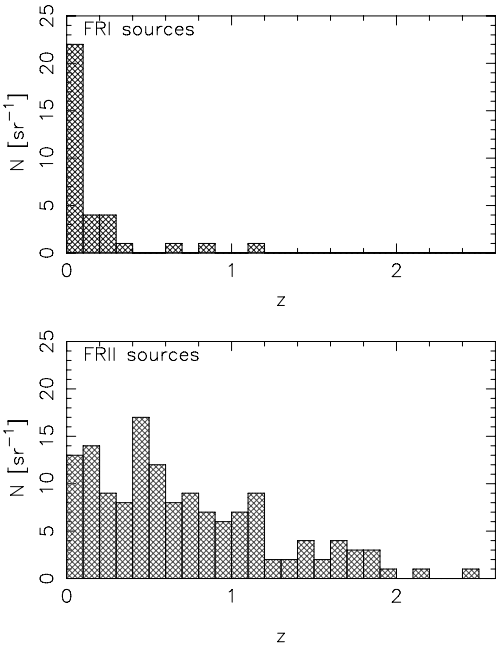

Figure 4. Redshift distributions for the CoNFIG sample. Details are given in Table 4. The FRI distribution is concentrated at low redshifts ($z \leq 0.5$) while the FRII distribution lies over a wider range, up to $z \sim 2.5$.

Table 4. Redshift completeness in the CoNFIG and CoNFIG-2 samples. Redshift information was retrieved from the SIMBAD data base. CSS and unresolved sources from Table 2 are regrouped with compact and FRII sources, respectively.

	CoNFIG		
	FRI	FRII	Compact
With z	34	142	68
Per cent of group with z	94.4	90.4	83.9
Per cent of sample with z	12.4	51.8	24.8
	CoNFIG-2		
	FRI	FRII	Compact
With z	22	97	52
Per cent of group with z	81.5	65.1	77.6
Per cent of sample with z	9.0	39.9	21.4

Table 5. Redshift distribution information for the CoNFIG sample.

Type	Per cent of group with ID	Redshift			
		Min	Max	Mean	Median
All	79.6	0.0034	3.522	0.715	0.580
FRI	97.2	0.0034	1.191	0.157	0.053
FRII	75.1	0.0456	2.474	0.712	0.572
Compact	80.2	0.0336	3.5220	1.001	0.909

emitted at $\nu_{\rm rest} = 1.4$ GHz will correspond to an observed flux at frequency $\nu_{\rm obs} < 1.4$ GHz.

Values for spectral indices are listed in Table A. The median value is $\alpha = -0.67$. However, the extended sources are grouped around a median value of $\alpha = -0.73$ as seen in Fig. 5, while the compact sources, as is well known, show a broader distribution.

Fig. 6 presents the luminosity distributions for FRI and FRII objects. The distribution of FRII sources only (excluding unresolved

Table 6. Surveys used to retrieve flux density information.

Frequency	Survey	Reference
178 MHz	3C	Kellermann, Pauliny-Toth & Williams (1969)
	4C	Pilkington & Scott (1965)
365 MHz	Texas	Douglas et al. (1996)
408 MHz	Parkes	Wright & Otrupcek (1990)
	B3	Ficarra et al. (1985)
2.7 GHz	3C	Kellermann et al. (1969)
	Parkes	Wright & Otrupcek (1990)
5.0 GHz	3C	Kellermann et al. (1969)
	Parkes	Wright & Otrupcek (1990)
	MIT-Greenbank	Bennett et al. (1986)

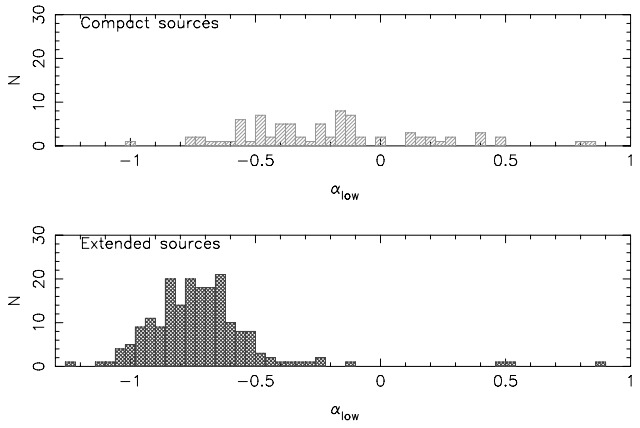

Figure 5. Spectral index distribution (using frequencies 178 MHz $\leq \nu \leq$ 1.4 GHz). The distribution peaks around -0.7, which is the usual value for extended sources, but has a long tail to flat/inverted spectra.

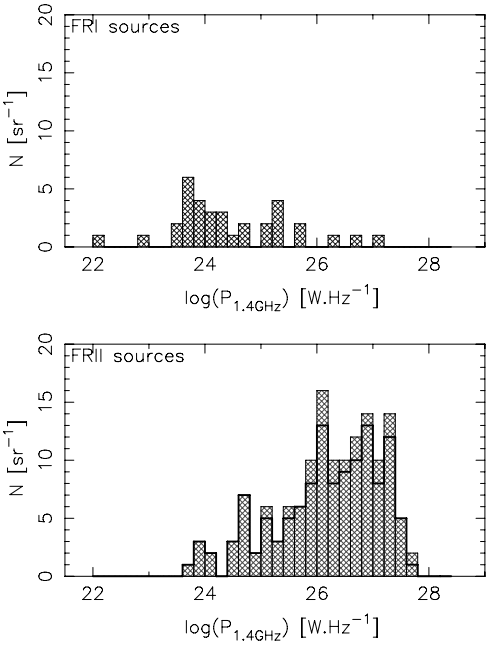

Figure 6. Luminosity distributions for FRI and FRII sources. The solid-line histogram in the FRII luminosity distribution plot corresponds to the distribution we would get if the unresolved sources were excluded from the FRII grouping.

sources) is shown as a solid-line distribution on the plot. As stated in Section 3.3, the inclusion of the unresolved sources with the FRII sources has very little effect on the structure of the distribution.

6 FRI/FRII SOURCE COUNTS

One of the challenges in modelling the space densities of FRI and FRII sources is to compute an accurate source count for each morphological type. This implies determining the morphological type of all sources used.

To increase the number of sources with morphology information, five samples at different flux density limits were combined with the CoNFIG sample. These samples include the CENSORS (Best et al. 2003) and BDFL (Bridle et al. 1972) samples, as well as the three extra CoNFIG samples (see details in Section 3.4 and Table 3). The morphologies of the sources in each sample were determined by looking at the FIRST and NVSS contour plots as described in Section 3 (with the exception of the CENSORS sources and some of the BDFL sources, as described in the next section).

6.1 The CENSORS and BDFL samples

6.1.1 The CENSORS sample

The CENSORS (Combined EIS–NVSS Survey Of Radio Sources) sample (Best et al. 2003; Brookes et al. 2005, 2007) contains 150 sources complete to $S_{1.4\,\mathrm{GHz}} = 7.2$ mJy, selected from NVSS over the ESO Imaging Survey (EIS) Patch D. The sample has a median flux density of $S_{1.4\,\mathrm{GHz}} \sim 15$ mJy and optical identifications for 68 per cent of the sources.

The wide field EIS comprises a relatively wide-angle survey of four distinct patches of sky up to 6 deg^2 each (Nonino et al. 1999). Patch D is the most northerly, with a limiting magnitude of $I \sim 23$ (Benoist et al. 1999) and an area of 2×3 deg^2 centred on $09^{\mathrm{h}}51^{\mathrm{m}}36\overset{\mathrm{s}}{.}0\ -21^{\circ}00'00''$ (J2000).

The goals of the CENSORS sample (Best et al. 2003) are to constrain evolution of the top end of the black hole mass function, study the environments around radio sources at different luminosities, test the K–z relation for radio sources and test the dual-population models.

Little classification of the CENSORS sources has been done, although Brookes et al. (2007) presented a list of the possible RQSOs. To attempt a preliminary morphological classification, we used the NVSS images to determine the morphology of the sources; in most cases though, the resolution is far too low to determine the morphology of the extended sources. In the case of the CoNFIG sample, this was solved by using FIRST images together with supplementary VLA observations. However, the CENSORS sample does not overlap with the FIRST survey, or any other higher resolution samples. Ledlow & Owen (1996) showed that FRI and FRII sources are separated on a radio power–optical magnitude diagram. Following this idea, we used radio flux densities and B magnitude data from CoNFIG and CoNFIG-2 to determine a line in the radio power–optical B magnitude diagram below which FRI morphology dominates. The line is defined as (as shown in Fig. 7)

$$\log P_{1.4\ \mathrm{GHz}} = -0.27 M_B + 18.8. \quad (3)$$

This relation was then applied to the 136 sources from CENSORS using the flux density and magnitude information from Best et al. (2003), using a K-correction value of $K_{\mathrm{corr}} = 1.122\,z$. As a result, 49 sources were classified as FRI and 87 as FRII. Note that, for 63 CENSORS sources, B magnitude information were not available and a B–z relation similar to the R–z relation defined in Section 4 was then used to determine M_B.

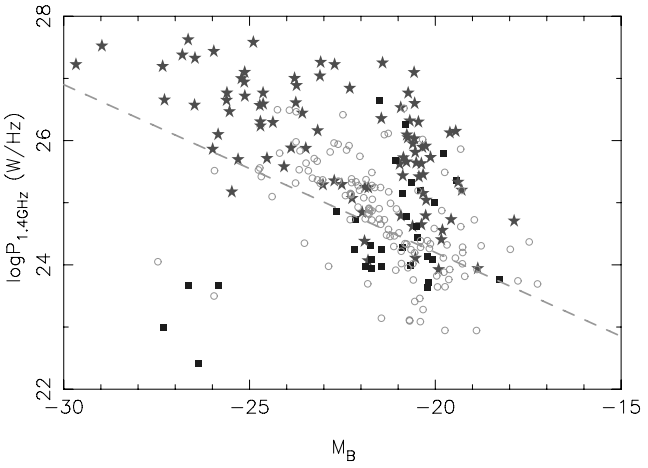

Figure 7. Radio power–optical B magnitude relation for the CoNFIG and CoNFIG-2 sources. FRIs (filled squares) seem to take over FRIIs (stars) below the dash line $\log P_{1.4\,\mathrm{GHz}} = -0.27 M_B + 18.8$. This relation is used to determine the FRI/FRII classification for non-QSO sources from CENSORS (open circles).

6.1.2 The BDFL sample

The BDFL sample (Bridle et al. 1972) contains 424 sources and is complete to $S_{1.4\,\mathrm{GHz}} \geq 1.7$ Jy in the area of sky $-5^{\circ} < \delta < +70^{\circ}$, $|b| > 5^{\circ}$.

To improve definition of the high flux density ends of the morphological source counts, sources from this sample with $S_{1.4\,\mathrm{GHz}} \geq 4.0$ Jy were selected, yielding a total number of 90 sources. The morphology of each source was determined from either Laing et al. (1983) or Kharb & Shastri (2004), or by looking at the NVSS contours. As a result, of the 90 sources, 21 sources are classified as FRI, 38 as FRII and 31 as compact.

6.2 Compiling the source count

In total, there are ∼500 sources from the combined BDFL (down to 4.0 Jy), CENSORS (at 7.2 mJy) and CoNFIG (at 1.3 Jy) samples. Still, as illustrated in Fig. 8, large areas of the P–z plane are not covered.

To improve coverage, the three other CoNFIG samples described in Section 3.4 were used. In all three of these samples, sources with $S_{1.4\,\mathrm{GHz}} \geq 1.3$ Jy were removed as they are already present in the CoNFIG sample.

The relative differential source counts $\Delta N/\Delta N_0$ for FRI and FRII sources were then computed from the combined sample of 244 FRI and 736 FRII sources. Data for the source count presented in Fig. 9 can be found in Table B3.

It is seen that FRII sources dominate the total count, except at low flux densities ($\log S_{1.4\,\mathrm{GHz}} \lesssim -1.6$), where the FRI sources suddenly take over. Since most of the FRI count at low flux densities is composed of low-luminosity sources at low redshift, our results show that FRI objects must undergo some mild evolution. This is consistent with the results of Sadler et al. (2007), who studied low power sources in the 2SLAQ survey (Richards et al. 2005) and found evidence that FRIs undergo significant evolution over $0 < z < 0.7$. Our results also show that FRIs undergo less evolution

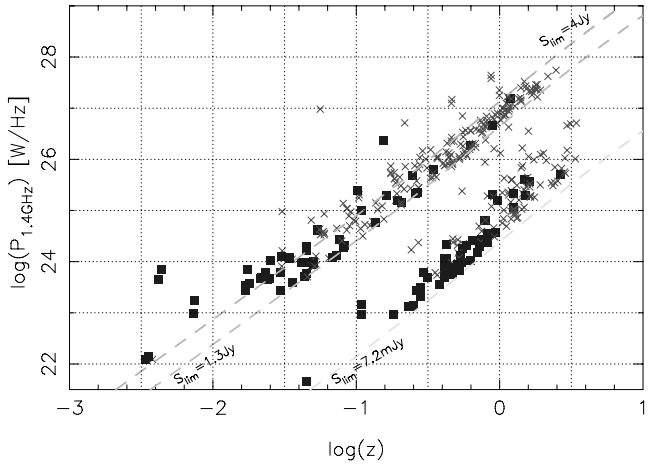

Figure 8. *P–z* plane for the CoNFIG sources. FRIs and FRIIS are represented by squares and crosses, respectively. The flux-density limit lines for the BDFL (down to 4.0 Jy), CENSORS (at 7.2 mJy) and CoNFIG (at 1.3 Jy) samples are represented as dashed lines, respectively. The plane is divided into sections of $\Delta\log(P) = 1$ and $\Delta\log(z) = 0.5$ to illustrate the poor coverage of some regions.

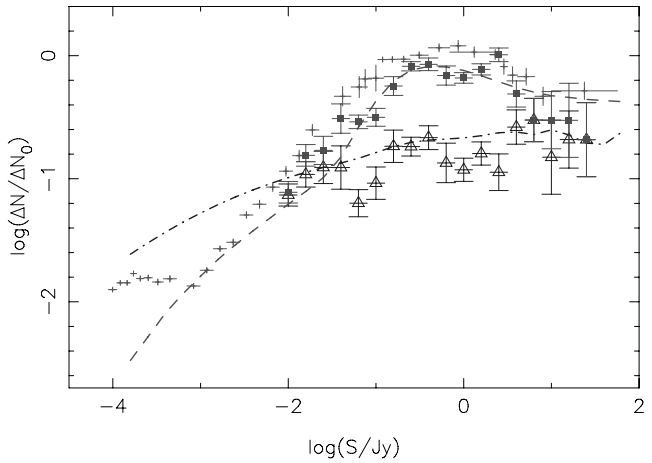

Figure 9. Relative differential source count for FRI (triangles) and FRII (squares) sources. A 1.4-GHz source count, compiled from the data of Bridle et al. (1972), Machalski (1978), Hopkins et al. (2003) and Prandoni et al. (2001), is represented by the grey crosses for comparison. Here, $\Delta N_0 = 200\Delta(S^{-1.5})$ and the error bars correspond to $\sqrt{N}$ where N is the number of objects in each bin. The counts are fitted by an illustrative model (FRI: dot–dashed line, FRII: dashed line), the details of which are described in Section 6.2. The FRII sources mostly dominate the count, except at low flux densities, where FRI sources take over. Our results show that FRI objects must undergo some mild evolution and that many of the mJy sources are radio galaxies, mostly FRIs.

than FRIIs, and they do not participate much in the source count 'evolution bump' around $S_{1.4\,\mathrm{GHz}} \sim 1$ Jy. This is in agreement with previous investigations stretching back to Longair (1966).

An illustrative exponential evolution model of space density, as described by Wall et al. (1980), was used to fit the data, as shown in Fig. 9. In the case of both FRI and FRII sources, the luminosity distribution obtained for the CoNFIG sample was used as starting points. This approach, as detailed in Wall et al. (1980), assumes that the luminosity function $\rho(P, z)$ can be factorized as $\rho(P, z) = F(P, z)\rho_0(P)$, where $\rho_0(P)$ is the local luminosity function and $F(P, z)$ an evolution function transforming $\rho_0(P)$ into the redshift and luminosity-dependent $\rho(P, z)$. The details of the evolution function $F(P, z)$ successfully fitting the two morphology counts (with the same set of parameters) are as follows:

$$F(P,z) = \begin{cases} \mathrm{e}^{M(P)\tau} & z \le z_\mathrm{c}, \\ 0 & z > z_\mathrm{c}, \end{cases} \tag{4}$$

where z_c is the redshift cut-off (maximum redshift at which a population exists) and τ is the look-back time

$$\tau = \frac{1}{H_0}\int_0^z \frac{\mathrm{d}z'}{(1+z)\sqrt{\Omega_\mathrm{M}(1+z)^3 + \Omega_\mathrm{K}(1+z)^2 + \Omega_\Lambda}} \tag{5}$$

with *M(P)* defined as

$$M = \begin{cases} M_1 & P < P_1, \\ \frac{(M_2-M_1)(\log P_1 - \log P)}{\log P_1 - \log P_2} + M_1 & P_1 \le P \le P_2, \\ M_2 & P > P_2. \end{cases} \tag{6}$$

The best-fitting values for this model are $z_\mathrm{c} = 4.37$, $M_1 = 2.38$, $M_2 = 11.63$, $\log P_1 = 26.0$ and $\log P_2 = 26.9$.

This is only an illustrative model. Accurate modelling of the FRI/FRII source counts and luminosity functions will be the subject of a future study.

The morphological counts and the model fit raise two points.

(1) If a single model, albeit one with differential evolution, can describe both populations, are the populations separate, or necessarily one (Snellen & Best 2001; Rigby et al. 2007)? At present the question is a semantic one: we do not have an immediate hypothesis to test requiring FRIs and FRIIs to be one population or two. What is of interest in this is whether FRIs and FRIIs at the same radio luminosity show exactly the same evolution, and our single model successfully fitting the data suggests that they do. This question will be examined in more detail in subsequent analyses.

(2) Our model is a hands-off best fit to the composite and morphologically divided source counts at 1.4 GHz – down to 10 mJy. It is not a valid model, because it predicts far too many sources in total at lower flux densities. A valid model needs a rapid downturn to be achieved at about 0.01 Jy, and it must be that further modelling details need introducing to achieve this. What seems clear however is that a large proportion of sources at a level of 1 mJy (i.e. at 'mJy corner') must be FRIs. In fact starburst galaxies are usually thought to account for the sub-mJy part of the source count. However, analysis of several radio sources from the VLA–CDFS survey by Padovani et al. (2007) shows that over two-thirds of the sub-mJy sources are faint radio galaxies, mostly FRIs. Our results support this finding. The next paper of this short series will examine the combined data and space density models in more detail.

7 SUMMARY

The CoNFIG sample is constructed as a sample of 274 radio sources from NVSS with $S \ge 1.3$ Jy. Redshift information is available for ∼80 per cent of the sample, and morphological classifications were obtained for all of the sources, either from NVSS and FIRST contour plots, or, for 46 sources, from 8-GHz VLA observations. These data allow us to compute morphology-dependent luminosity distributions and source counts.

To increase the number of sources with morphology information, three more samples were constructed in subareas of the main region with flux density limits of 0.8, 0.2 Jy and 50 mJy. Morphological identifications were obtained only from NVSS and FIRST contour plots for those sources. Morphological information for the

CENSORS and BDFL sample were obtained from the Ledlow–Owen relation between radio power and optical magnitude and from published classification, respectively. Combining these six samples allowed us to compile source counts for FRI and FRII sources separately. A simple, single evolution model for space density was then fitted to these data.

Our data show mild evolution of the FRI sources at low redshift; however, they do not participate in the 'evolution bump' around $S_{1.4\,\mathrm{GHz}} \sim 1$ Jy. The results also support the observation that a large number of mJy sources are FRIs galaxies and not starburst galaxies as previously assumed.

ACKNOWLEDGMENTS

We are very grateful to Jim Dunlop for many helpful suggestions, and to Rick Perley and Eric Greison for their precious help with the VLA observation and data reduction. We also thank the referee for very helpful comments.

This work was supported by the National Sciences and Engineering Research Council of Canada.

The National Radio Astronomy Observatory is a facility of the National Science Foundation operated under cooperative agreement by Associated Universities, Inc. This research has made use of the SIMBAD data base, operated at CDS, Strasbourg, France.

REFERENCES

Abazajian K. et al., 2003, AJ, 126, 2081
Abazajian K. et al., 2004, AJ, 128, 502
Abazajian K. et al., 2005, AJ, 129, 1755
Adelman-McCarthy J. K. et al., 2006, ApJ, 162, 38
Baars J. W. M., Genzel R., Pauliny-Toth I. I. K., Witzel A., 1977, A&A, 61, 99
Barkhouse W. A., Hall P. B., 2001, AJ, 121, 2843
Barthel P. D., 1989, ApJ, 336, 606
Bauer F., Condon J. J., Thuan T. X., Broderick J. J., 2000, ApJS, 129, 547
Baum S. A., Heckman T. M., 1989, ApJ, 336, 681
Baum S. A., Zirbel E. L., O'Dea C. P., 1995, ApJ, 451, 88
Beasley A. J., Gordon D., Peck A. B., Petrov L., MacMillan D. S., Fomalont E. B., Ma C., 2002, ApJS, 141, 13
Beckmann V., Gehrels N., Shrader C. R., Soldi S., 2006, ApJ, 638, 642
Bennett C. L.,Lawrence C. R., Burke B. F., Hewitt J. N., Mahoney J., 1986, Astron. J. Suppl., 61, 1
Benoist C. et al., 1999, A&A, 346, 58
Best P. N., Arts J. N., Röttgering H. J. A., Rengelink R., Brookes M. H., Wall J., 1999, MNRAS, 310, 223
Best P. N., Arts J. N., Röttgering H. J. A. et al., 2003, MNRAS, 346, 627
Blundell K. M., Rawlings S., 2001, ApJ, 562, L5
Bongiovanni A., Bruzual G., Magris G., Gallego J., García-Dabó C. E., Coppi P., Sabbey C., 2005, MNRAS, 359, 930
Bower R. G., Benson A. J., Malbon R., Helly J. C., Frenk C. S., Baugh C. M., Cole S., Lacey C. G., 2006, MNRAS, 370, 645
Brinkmann W., Siebert J., Reich W., Fuerst E., Reich P., Voges W., Truemper J., Wielebinski R., 1995, A&AS, 109, 147
Bridle A. H., Davis M. M., Fomalont E. B., Lequeux J., 1972, AJ, 77, 1401
Brookes M. H., Best P. N., Rengelink R., Röttgering H. J., 2005, MNRAS, 00, 1
Brookes M. H., Best P. N., Peacock J. A., Röttgering H. J. A., Dunlop J. S., 2007, MNRAS, 385, 1297
Brown M. J. I., Webster R. L., Boyle B. J., 2001, AJ, 121, 2381
Cannon R. et al., 2006, MNRAS, 372, 425
Capetti A., Fanti R., Parma P., 1995, A&A, 300, 643
Cappi A., Benoist C., da Costa L. N., 2003, A&A, 408, 905
Clewley L., Jarvis M. J., 2004, MNRAS, 352, 909
Colless M. et al., 2001, MNRAS, 328, 1039
Condon J. J., Cotton W. D., Greisen E. W., Yin Q. F., Perley R. A., Taylor G. B., Broderick J. J., 1998, ApJ, 115, 1693
Cowie L. L., Songaila A., Hu E. M., Cohen J. G., 1996, AJ, 112, 839
Croom S. M., Smith R. J., Boyle B. J., Shanks T., Miller L., Outram P. J., Loaring N. S., 2004, MNRAS, 349, 1397
Daly R. A., Djorgovski S. G., 2004, ApJ, 612, 652
de Grijp M. H. K., Keel W. C., Miley G. K., Goudfrooij P., Lub J., 1992, A&A, 96, 389
Douglas J. N., Bash F. N., Bozyan F. A., Torrence G. W., Wolfe C., 1996, AJ, 111, 1945
Dunlop J. S., Peacock J. A., 1990, MNRAS, 247, 19
Ellingson E., Yee H. K. C., 1994, ApJ, 92, 33
Enya K., Yoshii Y., Kobayashi Y., Minezaki T., Suganuma M., Tomita H., Peterson B. A., 2002, ApJ, 141, 23
Falcke H., Gopal-Krishna, Biermann P. L., 1995, A&A, 298, 395
Falco E. E. et al., 1999, PASP, 111, 438
Fanaroff B. L., Riley J. M., 1974, MNRAS, 167, 31P
Fanti C., Fanti R., 1994, in Bicknell G. V., Dopita M. A., Quinn P. J., eds, ASP Conf. Ser. Vol. 54, The First Stromlo Symposium: The Physics of Active Galaxies. Astron. Soc. Pac., San Francisco, p. 341
Fomalont E. B., Petrov L., MacMillan D. S., Gordon D., Ma C., 2003, AJ, 126, 2562
Gandhi P., Fabian A. C., Crawford C. S., 2006, MNRAS, 369, 1566
Gawronski M. P., Marecki A., Kunert-Bajraszewska M., Kus A. J., 2006, A&A, 447, 63
Gopal-Krishna, Wiita P. J., 2000, A&A, 363, 507
Gopal-Krishna, Ledoux C., Melnick J., Giraud E., Kulkarni V., Altieri B., 2005, A&A, 436, 457
Gregory S. A., Burns J. O., 1982, ApJ, 255, 373
Granato G. L., Silva L., Monaco P., Panuzzo P., Salucci P., De Zotti G., Danese L., 2001, MNRAS, 324, 757
Grimes J. A., Rawlings S., Willott C. J., 2005, MNRAS, 359, 1345
Hambly N. C., Irwin M. J., MacGillivray H. T., 2001, MNRAS, 326, 1279
Hardcastle M. J., Evans D. A., Croston J. H., 2006, MNRAS, 370, 1893
Heckman T. M., O'Dea C. P., Baum Stefi A., Laurikainen E., 1994, ApJ, 428, 65
Herbig T., Readhead A. C. S., 1992, ApJ, 81, 83
Hewett P. C., Folts C. B., Chaffee F. H., 2001, AJ, 122, 518
Hewitt A., Burbidge G., 1989, ApJ, 69, 1
Hewitt A., Burbidge G., 1991, ApJ, 75, 297
Heywood I., Blundell K. M., Rawlings S., 2007, MNRAS, 381, 1093
Hill G. J., Lilly S. J., 1991, ApJ, 367, 1
Hill G. J., Goodrich R. W., Depoy D. L., 1996, ApJ, 462, 163
Holt J., Tadhunter C. N., Morganti R., 2003, MNRAS, 342, 227
Hopkins A. M., Afonso J., Chan B., Cram L. E., Georgakakis A., Mobasher B., 2003, AJ, 125, 465
Jackson C. A., Wall J. V., 1999, MNRAS, 304, 160
Jones D. L., Preston R. A., 2001, AJ, 122, 2940
Kaiser C. R., Alexander P., 1997, MNRAS, 286, 215
Kaiser C. R., Best P. N., 2007, MNRAS, 381, 1548
Kellermann K. I., Pauliny-Toth I. I. K., Williams P. J. S., 1969, ApJ, 157, 1
Kharb P., Shastri P., 2004, A&A, 425, 825
Klamer I. J., Ekers R. D., Sadler E. M., Hunstead R. W., 2004, ApJ, 612, 97
Kovalev Y. Y., Nizhelsky N. A., Kovalev Yu. A., Berlin A. B., Zhekanis G. V., Mingaliev M. G., Bogdantsov A. V., 1999, A&AS, 139, 545
Kovalev Y. Y., Petrov L., Fomalont E. B., Gordon D., 2007, AJ, 133, 1236
Lahulla J. E., Merighi R., Vettolani G., Vigotti M., 1991, A&AS, 88, 525
Laing R. A., 1994, in Bicknell G. V., Dopita M. A., Quinn P. J., eds, ASP Conf. Ser. Vol. 54, The Physics of Active Galaxies. Astron. Soc. Pac., San Francisco, p. 201
Laing R. A., Riley J. M., Longair M. S., 1983, MNRAS, 204, 151
Lara L., Cotton W. D., Feretti L., Giovannini G., Marcaide J. M., Márquez I., Venturi T., 2001, A&A, 370, 409
Ledlow M. J., Owen F. N., 1996, ApJ, 112, 9
Liu F. K., Zhang Y. H., 2002, A&A, 381, 757
Longair M. S., 1966, MNRAS, 133, 421

Lu N. Y., Hoffman G. L., Groff T., Roos T., Lamphier C., 1993, ApJS, 88, 383
Machalski J., 1978, A&A, 65, 157
Machalski J., 1998, A&AS, 128, 153
Madore B. F., Helou G., Corwin H. G., Jr., Schmitz M., Wu X., Bennett J., 1992, in Worrall D. M., Biemesderfer C., Barnes J., eds, ASP Conf. Ser. Vol. 25, Astronomical Data Analysis Software and Systems I. Astron. Soc. Pac., San Francisco, p. 47
Marcha M. J. M., Browne I. W. A., 1995, MNRAS, 275, 951
Marcha M. J. M., Browne I. W. A., Impey C. D., Smith P. S., 1996, MNRAS, 281, 425
Marzke R. O., Huchra J. P., 1996, AJ, 112, 1803
Masson C. R., Wall J. V., 1977, MNRAS, 180, 193
Mathez G., 1969, A&A, 3, 127
Maxfield L., Thompson D., Djorgovski S., Vigotti M., Grveff G., 1995, PASP, 107, 369
Miller N. A., Ledlow M. J., Owen F. N., Hill J. M., 2002, AJ, 123, 3018
Nilsson K., 1998, A&A, 132, 31
Nonino M. et al., 1999, A&AS, 137, 51
Owen F. N., Ledlow M. J., 1994, in Bicknell G. V., Dopita M. A., Quinn P. J., eds, ASP Conf. Ser. Vol. 54, The Physics of Active Galaxies. Astron. Soc. Pac., San Francisco, p. 319
Owen F. N., Ledlow M. J., Keel W. C., 1995, AJ, 109, 140
Padovani P., Mainieri V., Tozzi P., Kellermann K. I., Fomalont E. B., Miller N., Rosati P., Shaver P., 2007, in Afonso J., Ferguson H. C., Mobasher B., Norris R., eds, ASP Conf. Ser. Vol. 380, At the Edge of the Universe: Latest Results from the Deepest Astronomical Surveys. Astron. Soc. Pac., San Francisco, p. 205
Parma P. et al., 1992, in Burgarella D., Livio M., O'Dea C., eds, Astrophysical Jets, Poster Papers from the Space Telescope Science Institute Symposium. STScI, Baltimore, p. 30
Peacock J. A., 1987, in Kundt W., ed., Astrophysical Jets and Their Engines. Reidel, Dordrecht, p. 185
Pearson T. J., Readhead A. C. S., 1988, ApJ, 328, 114
Petrov L., Kovalev Y. Y., Fomalont E., Gordon D., 2005, AJ, 129, 1163
Petrov L., Kovalev Y. Y., Fomalont E. B., Gordon D., 2006, AJ, 131, 1872
Pihlstroem Y. M., Conway J. E., Vermeulen R. C., 2003, A&A, 404, 871
Pilkington J. D. H., Scott P. F., 1965, MNRAS, 69, 183
Pinkney J., Burns J. O., Ledlow M. J., Gómez P. L., Hill J. M., 2000, AJ, 120, 2269
Polatidis A. G., Conway J. E., 2003, Publ. Astron. Soc. Aust., 20, 69
Polatidis A. G., Wilkinson P. N., Xu W., Readhead A. C. S., Pearson T. J., Taylor G. B., Vermeulen R. C., 1995, ApJ, 98, 1
Prandoni I., Gregorini L., Parma P., de Ruiter H. R., Vettolani G., Wieringa M. H., Ekers R. D., 2001, A&A, 365, 392
Quilis V., Bower R. G., Balogh M. L., 2001, MNRAS, 328, 1091
Rawlings S., Saunders R., Eales S. A., Mackay C. D., 1989, MNRAS, 240, 701
Richards G. T. et al., 2005, MNRAS, 360, 839
Rigby E. E., Best P. N., Snellen I. A. G., 2008, MNRAS, 385, 310
Rines K., Geller M. J., Kurtz M. J., Diaferio A., Jarrett T. H., Huchra J. P., 2001, ApJ, 561, 41
Roche N., Eales S., Hippelein H., 1998, MNRAS, 295, 946
Ryabinkov A. I., Kaminker A. D., Varshalovich D. A., 2003, A&A, 412, 707
Sadler E. M. et al., 2007, MNRAS, 381, 211
Saripalli L., Gopal-Krishna & Reich W., 1986, A&A, 170, 20
Scheuer P. A. G., 1987, in Zensus J. A., Pearson T. J., eds, Superluminal Radio Sources. Cambridge Univ. Press, Cambridge, p. 104
Schmidt M., 1976, ApJ, 209, 55
Schneider D. P. et al., 2001, A&A, 198, 7801
Schneider D. P. et al., 2005, AJ, 130, 367
Schneider D. P. et al., 2007, AJ, 134, 102
Silk J., Rees M. J., 1998, A&A, 331, 1
Singal A. K., 1993, MNRAS, 263, 139
Smith H. E., Smith E. O., Spinrad H., 1976, PASP, 88, 621
Smith R. J., Lucey J. R., Hudson M. J., Schlegel D. J., Davies R. L., 2000, MNRAS, 313, 469
Snellen I. A. G., Best P. N., 2001, MNRAS, 328, 897
Snellen I. A. G., McMahon R. G., Hook I. M., Browne I. W. A., 2002, MNRAS, 329, 700
Spinrad H., Marr J., Aguilar L., Djorgovski S., 1985, PASP, 97, 932
Stickel M., Kuehr H., 1994a, A&A, 103, 349
Stickel M., Kuehr H., 1994b, A&A, 105, 67
Stickel M., Fried J. W., Kuehr H., 1993, A&AS, 98, 393
Strom R. G., Riley J. M., Spinrad H., van Breugel W. J. M., Djorgovski S., Liebert J., McCarthy P. J., 1990, A&A, 227, 19
Thimm G. J., Roeser H. J., Hippelein H., Meisenheimer K., 1994, A&A, 285, 785
Thompson D. J., Djorgovski S., de Carvalho R., 1990, PASP, 102, 1235
Tinti S., de Zotti G., 2006, A&A, 445, 889
Trager S. C., Faber S. M., Worthey G., Gonzlez J. J., 2000, AJ, 119, 1645
Urry C. M., Padovani P., 1995, PASP, 107, 803
van Breugel W. J. M., Dey A., 1993, ApJ, 414, 563
van Breugel W., Fragile C., Croft S., de Vries W., Anninos P., Murray S., 2004, in Storchi-Bergmann T. H. L. C., Schmitt H. R., eds, Proc. IAU Symp. 222, The Interplay among Black Holes, Stars and ISM in Galactic Nuclei. Cambridge Univ. Press, Cambridge, p. 485
Vermeulen R. C., Taylor G. B., 1995, AJ, 109, 1983
Wall J. V., Jackson C. A., 1997, MNRAS, 290, 17
Wall J. V., Pearson T. J., Longair M. S., 1980, MNRAS, 193, 683
Wang J. C. L., Sulkanen M. E., Lovelace R. V. E., 1992, ApJ, 390, 46
Wegner G. et al., 2001, AJ, 122, 2893
White R. L., Becker R. H., Helfand D. J., Gregg M. D., 1997, ApJ, 475, 479
Wills D., Wills B. J., 1976, ApJS, 31, 143
Willott C. J., Rawlings S., Blundell K. M., Lacy M., 2001, MNRAS, 322, 536
Willott C. J., Rawlings S., Archibald E. N., Dunlop J. S., 2002, MNRAS, 331, 435
Willott C. J., Rawlings S., Jarvis M. J., 2000, MNRAS, 313, 237
Wills D., Wills B. J., 1976, ApJ, 31, 63
Woo J., Urry C. M., van der Marel R. P., Lira P., Maza J., 2005, ApJ, 631, 762
Wright A., Otrupcek R., 1990, PASP, 41, 47
Xu W., Lawrence C. R., Readhead A. C. S., Pearson T. J., AJ, 108, 395
Zensus J. A., Ros E., Kellermann K. I., Cohen M. H., Vermeulen R. C., Kadler M., 2002, AJ, 124, 662

SUPPORTING INFORMATION

Additional Supporting Information may be found in the online version of this article.

Appendix A. CoNFIG sample.
Appendix B. CoNFIG-2, CoNFIG-3 and CoNFIG-4 samples.
Appendix C. Contour plots.
Appendix D. VLA observations.

Please note: Wiley-Blackwell are not responsible for the content or functionality of any supporting materials supplied by the authors. Any queries (other than missing material) should be directed to the corresponding author for the article.

This paper has been typeset from a TEX/LATEX file prepared by the author.